

# Pumping of nuclear spins by the optical solid effect in a quantum dot

E. A. Chekhovich<sup>1,2</sup>, M. N. Makhonin<sup>1</sup>, K. V. Kavokin<sup>1,3</sup>, A. B. Krysa<sup>4</sup>, M. S. Skolnick<sup>1</sup>, A. I. Tartakovskii<sup>1</sup>

<sup>1</sup>*Department of Physics and Astronomy, University of Sheffield, Sheffield S3 7RH, UK*

<sup>2</sup>*Institute of Solid State Physics, 142432, Chernogolovka, Russia*

<sup>3</sup>*A. F. Ioffe Physico-Technical Institute, 194021, St. Petersburg, Russia*

<sup>4</sup>*Department of Electronic and Electrical Engineering, University of Sheffield, Sheffield S1 3JD, UK*

(Dated: November 14, 2018)

We demonstrate that efficient optical pumping of nuclear spins in semiconductor quantum dots (QDs) can be achieved by resonant pumping of optically "forbidden" transitions. This process corresponds to one-to-one conversion of a photon absorbed by the dot into a polarized nuclear spin, which also has potential for initialization of hole spin in QDs. Pumping via the "forbidden" transition is a manifestation of the "optical solid effect", an optical analogue of the effect previously observed in electron spin resonance experiments in the solid state. We find that by employing this effect, nuclear polarization of 65% can be achieved, the highest reported so far in optical orientation studies in QDs. The efficiency of the spin pumping exceeds that employing the allowed transition, which saturates due to the low probability of electron-nuclear spin flip-flop.

PACS numbers:

Resonant optical pumping is a powerful method for direct control of individual quantum states in a variety of physical systems [1, 2] now also including semiconductor quantum dots [3, 4, 5, 6, 7, 8, 9, 10]. In III-V semiconductor nano-structures the optically controlled carrier spin dynamics are strongly influenced by the hyperfine coupling of the electron spin with a bath of nuclei. The hyperfine interaction (HI) is at the core of the resonant optical pumping of the hole spin in charged dots [5, 9]. On the other hand, the HI shortens the electron spin coherence and lifetime [11, 12] and therefore is unfavorable for electron spin manipulation in nano-structures [10, 13, 14]. Such undesirable effects arising from fluctuations of the effective nuclear magnetic field can be suppressed by locking optical transitions in the dot to a resonant laser [10, 15], or by pumping nuclear spins into a suitable narrow distribution of states [13, 16]. Another widely discussed approach is to pump very high nuclear spin polarizations [17], a task so far eluding an experimental realization.

Here we present experiment and theory demonstrating that excitation of a positively charged dot with light resonant with an optically forbidden transition leads to the most efficient nuclear polarization in QDs, exceeding that achievable by the well-studied optical spin pumping employing allowed transitions. This counter-intuitive observation sheds new light on the long standing problem of the realization of large nuclear polarization in semiconductors. Both non-resonant excitation and resonant pumping via the allowed transition, leading to the well-understood Overhauser effect, rely on high occupancy of a spin-polarized trion on the dot. They saturate with saturation of the optical transition at a relatively small spin pumping efficiency, limited by the low probability of the electron-nuclear spin flip-flop. In contrast, pumping via the spin-forbidden transition, enabled by electron spin state mixing due to the HI [18], relies only on the

presence of a hole. Its efficiency is only limited by the radiative recombination rate of the trion. This process, revealed in our work, arises from absorption of a single photon accompanied by the simultaneous spin flip of an electron and a single nucleus. This is a close analogue of the "solid effect" [19, 20], a dynamic nuclear polarization phenomenon observed in solids with paramagnetic centers under microwave excitation. By employing the "optical solid effect" we find that nuclear polarization increases with the laser intensity and saturates when the polarization degree reaches 65%, the highest reported so far for QDs [21, 22, 23]. We show that this is not a result of saturation of the optical transition itself, but rather may be a limitation due to inherent properties of the interacting electron-nuclear spin system, setting a fundamental limit to the maximum polarization achievable by optical pumping. The one-to-one photon-to-polarized-nucleus conversion can also serve as a one-step initialization of the hole spin.

The sample containing InP/GaInP QDs was grown by metal-organic vapor phase epitaxy (see details in Ref. [23]). The experiments were performed on individual dots at a temperature of 4.2 K, in external magnetic field  $B_z$  up to 8 T perpendicular to the sample surface. We study positively charged QDs emitting at  $\sim 1.84$  eV. The sample was not intentionally doped. The dot charging with holes, verified by magneto-spectroscopy and Hanle effect measurements, occurred due to residual doping.

The observation of nuclear spin pumping in this work has been realised using pump-probe techniques, where the effect of the resonant pump excitation is determined by monitoring the whole spectrum of the dot using a non-resonant probe, an important contrasting factor to the selective spectral probing used in absorption measurements [3, 5, 9, 10]. The pump-probe experiment cycle is shown schematically in Fig.1(a). A long circularly polarized pump pulse from a tunable single-mode laser

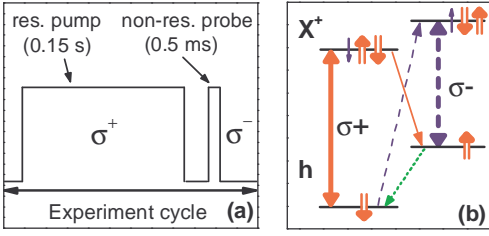


FIG. 1: (a) Pulse sequence used in the resonant nuclear spin pump-probe experiment. (b) Energy level diagram of a positively charged dot in magnetic field  $B_z$ . Electron and hole spin up (down) states are shown by  $\uparrow(\downarrow)$  and  $\uparrow(\downarrow)$  respectively. Long thick (thin) arrows show "allowed" ("forbidden") optical transitions. Dotted arrow shows hole spin relaxation.

excites the dot. A short pulse from a second laser, cross-circularly polarized relative to the pump and emitting below the GaInP band-gap at  $\sim 1.88$  eV, is used to excite photoluminescence (PL) from the positive trion  $X^+$  and to probe the states of the dot. The polarized PL excited by the probe pulse is analyzed with a 1 m double spectrometer. This enables absolute  $X^+$  transition energies to be determined and Overhauser fields for a given pump laser wavelength to be deduced. The duration of the probe pulse was chosen to eliminate its effect on the nuclear spin polarization on the dot: for most of the measurements we used 0.15 s and 0.5 ms pump and probe pulses, respectively. Multiple cycles were repeated for each resonant laser frequency to improve the signal to noise ratio, yielding a typical measurement time of 1 min, exceeding the time required for the nuclear polarization to reach its steady-state value ( $\tau_{build-up} \approx 10$  s).

A diagram of the energy levels of the positively charged dot in external magnetic field  $B_z$  is shown in Fig.1(b). The system ground state with hole spin up(down)  $|\uparrow\rangle(|\downarrow\rangle)$  and the photo-excited  $X^+$  trion state with electron spin up(down)  $|\uparrow\downarrow\rangle(|\uparrow\downarrow\rangle)$  have energies  $E_{\uparrow(\downarrow)} = \pm\mu_B g_h B_z/2$  and  $E_{\uparrow\downarrow\uparrow(\uparrow\downarrow\downarrow)} = E_{X^+} \pm \mu_B g_e (B_z + B_N)/2$  respectively, where  $\mu_B$  is the Bohr magneton,  $B_N$  is the nuclear field,  $g_{e(h)} \approx +1.5(+3.1)$  is the electron(hole) g-factor and  $E_{X^+}$  is the PL energy at  $B_z=B_N=0$ . Allowed  $\sigma^{-(+)}$  polarized optical transitions from  $|\uparrow\downarrow\rangle(|\uparrow\downarrow\rangle)$  to  $|\uparrow\rangle(|\downarrow\rangle)$  observed in PL are shown by thick arrows.

The effect of the resonant excitation with a  $\sigma^+$  polarized pump laser is demonstrated in Fig.2. Here the magnitude of the nuclear field  $B_N$  deduced from the  $X^+$  spectral splitting  $(E_{\uparrow\downarrow\downarrow} - E_{\downarrow\downarrow}) - (E_{\uparrow\downarrow\uparrow} - E_{\uparrow\uparrow})$  is shown as a function of the pump laser energy  $E_l$ .

As shown in Fig.2(a) for the case of high magnetic field  $B_z = 2.5$  T and laser power  $P_{res} = 15$   $\mu$ W, the dependence of  $B_N$  on laser frequency has the form of two strongly asymmetric dips. When the laser is tuned from low energy close to the resonance with the optically allowed transition  $|\downarrow\rangle \leftrightarrow |\uparrow\downarrow\rangle$ ,  $B_N$  decreases from 0 T to  $-0.6$  T and then switches abruptly to  $B_N \sim -0.2$  T

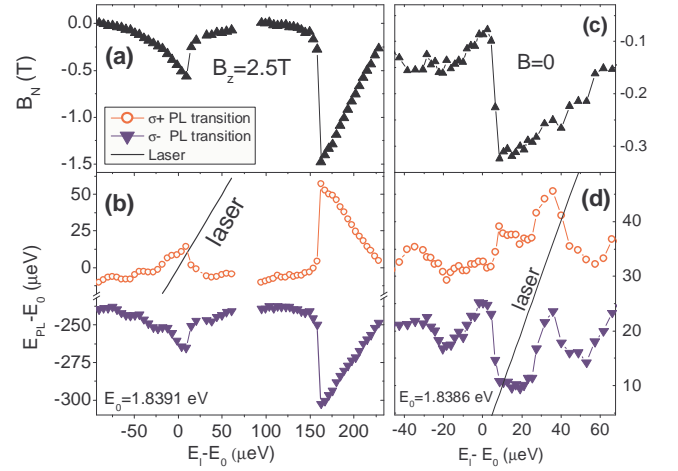


FIG. 2: Overhauser field  $B_N$  on the dot (a,c) and PL transitions energies  $E_{PL}$  (b,d) as a function of the energy  $E_l$  of the  $\sigma^+$  polarized resonant laser with excitation power  $P_{res}=15$   $\mu$ W at  $B_z=2.5$  T (a,b) and  $B_z=0$  (c,d). The full lines on panels (b,d) show the laser energy.

with a further slow increase to  $\sim 0$  T. Surprisingly, another strong decrease of  $B_N$  is observed when the laser is tuned near the spin-forbidden transition  $|\downarrow\rangle \leftrightarrow |\uparrow\downarrow\rangle$  [thin dashed arrow in Fig.1(b)]. Here in marked contrast, an abrupt change in  $B_N$  from 0 to  $-1.5$  T occurs at low laser energy, with the maximum  $|B_N|$  at this optical power 2.5 times larger than that excited via the spin-allowed transition. When  $E_l$  is tuned further,  $B_N$  gradually increases back to 0.

The results in Fig.2(a) are deduced from the measurement of absolute  $X^+$  PL transition energies shown in Fig.2(b) as a function of laser energy. The detuning between the  $\sigma^+$  PL line and the laser at each  $E_l$  is given by the energy difference between the circles and the black line in Fig.2(b), which represents the energy of the laser. In the case of the spin-allowed process the abrupt change of nuclear polarization occurs just as the laser is tuned slightly above the  $\sigma^+$  PL line.

The same laser tuning experiment was repeated at  $B=0$  [see Fig. 2(c) and (d)]. At  $B=0$  the shifts caused by nuclear polarization are comparable to random spectral diffusion of the dot PL energy, arising most likely from interaction with random charges in the surrounding matrix. An asymmetric form of the resonance similar to that in high magnetic fields can be seen in Fig.2(c). However, an abrupt change in  $B_N$  occurs only when the  $\sigma^+$  polarized laser comes into resonance with the  $\sigma^-$  polarized  $|\uparrow\rangle \leftrightarrow |\uparrow\downarrow\rangle$  PL transition coinciding with the forbidden  $|\downarrow\rangle \leftrightarrow |\uparrow\downarrow\rangle$  transition at  $B=0$ . Furthermore, the asymmetry of the resonance curve is similar to that observed for pumping via the spin-forbidden transition at  $B_z = 2.5$  T in Fig.2(a): the abrupt change in  $B_N$  is observed towards lower laser energy.

In order to explain the observed effects we consider the

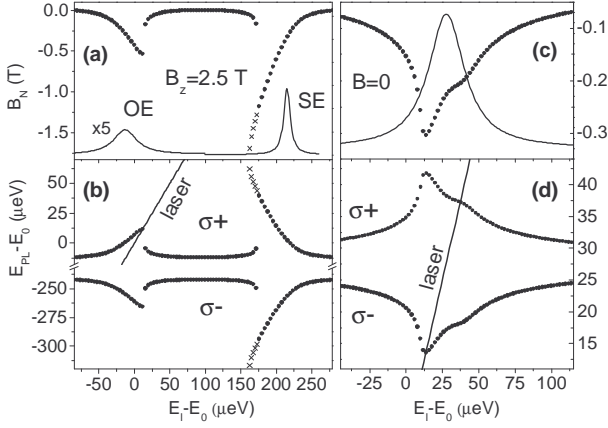


FIG. 3: (a) and (c) show calculated nuclear field  $B_N$  on the dot ([crosses]circles show [meta]stable solutions) and nuclear spin pumping rate  $|W_{OE} + W_{SE}|$  at  $B_N=0$  (lines). (b) and (d) show calculated PL transitions energies  $E_{PL}$  as a function of the energy  $E_l$  of the  $\sigma^+$  polarized laser at  $B_z=2.5$  (a,b) and  $B=0$  T (c,d). Lines on panels (b,d) show the laser energy.

resonant nuclear spin pumping mechanism illustrated in Fig.1(b). As the QD contains of the order of  $10^4$  magnetic nuclei, their polarization requires many cycles of optical excitation/recombination. The optically allowed circularly polarized transitions shown in Fig.1(b) with thick arrows conserve spin and cannot be responsible for nuclear spin pumping. For the  $\sigma^+$  polarized excitation used in Fig.2, there are two possible cyclic processes yielding nuclear polarization. Both start from the spin-down state of the resident hole  $|\downarrow\rangle$  and involve optically forbidden transitions:

(1) The cycle associated with the Overhauser effect (OE) consists of the following steps (i) excitation of the allowed transition to the spin-down  $|\uparrow\downarrow\rangle$  state [thick solid arrow in Fig. 1(b)]; (ii) recombination to the spin-up hole state  $|\uparrow\rangle$  (thin solid arrow), assisted by the hyperfine interaction (otherwise this transition is forbidden); (iii) hole spin-flip back into  $|\downarrow\rangle$  state (dotted arrow).

(2) The cycle associated with the optical solid effect (SE) also involves three steps: (i) hyperfine-interaction-assisted excitation of the spin-up  $|\uparrow\downarrow\rangle$  state via the spin-forbidden transition (thin dashed arrow); (ii)  $X^+$  recombination via the allowed transition into the  $|\uparrow\rangle$  state (thick dashed arrow); (iii) and, finally, the hole spin-flip completing the cycle.

Each of the above excitation cycles results in change of the  $Z$ -projection of the total nuclear spin in the QD by  $-1$ . We calculate the total rate of spin pumping into the nuclear system  $W_{pump}$  as the sum of the rates of these cycles by solving optical Bloch equations for the two photo-excitation paths.

For the SE cycle, the lifetime  $\tau$  of the excited state is determined by the allowed recombination transition. In contrast, for the OE cycle the recombination rate

into the spin-up hole state is reduced by the factor  $\alpha^2 = \mu_B^2 g_e^2 \langle \delta B_N^2 \rangle / E_{eZ}^2$  characterizing mixing of the two  $X^+$  states by the hyperfine interaction. Here  $\langle \delta B_N^2 \rangle$  is the mean squared fluctuation of the Overhauser nuclear field, while  $E_{eZ} = E_{\uparrow\downarrow\uparrow} - E_{\uparrow\downarrow\downarrow}$  is the electron Zeeman splitting characterizing the energy difference between  $X^+$  trion states. The hyperfine admixture factor  $\alpha$  also governs the optical matrix element for the excitation transition in the SE cycle, which is given by  $\alpha\Omega_R$  rather than  $\Omega_R$  as in the case of the OE cycle (here  $\Omega_R$  is the laser Rabi frequency). Note that in our experiments the splitting of the  $X^+$  states always exceeds by far the magnitude of the electron splitting due to the nuclear spin fluctuation  $\mu_B g_e \langle \delta B_N^2 \rangle^{1/2} \approx 1 \mu\text{eV}$ , and therefore  $\alpha$  remains small. As a result, we obtain the following expressions for the rates of OE and SE cycles:

$$W_{OE} = -\frac{\alpha^2 \tau^{-1} \cdot (\tau \Omega_R)^2 / 2}{1 + (\tau \Omega_R)^2 + (E_{\uparrow\downarrow\downarrow} - E_{\downarrow} - E_l)^2 \tau^2 \hbar^{-2}}$$

$$W_{SE} = -\frac{\tau^{-1} \cdot (\alpha \tau \Omega_R)^2 / 2}{1 + (\alpha \tau \Omega_R)^2 + (E_{\uparrow\downarrow\uparrow} - E_{\downarrow} - E_l)^2 \tau^2 \hbar^{-2}}. \quad (1)$$

At low pumping ( $\tau \Omega_R \ll 1$ ) both processes result in identical resonance lineshape, shifted in energy by the splitting of the  $X^+$  states. However, with increasing pump intensity ( $\tau \Omega_R \approx 1$ ),  $W_{OE}$  saturates and broadens, while  $W_{SE}$  continues to grow linearly with pump intensity up to  $\tau \Omega_R \approx \alpha^{-1} \gg 1$ . Thus the overall efficiency of the SE process can exceed that of the OE by a factor of  $1/\alpha^2$ .

The stationary value of the nuclear field is found from the condition that the total pumping rate  $W_{pump}$  via SE and OE processes must equal the loss rate of nuclear polarization:

$$W_{OE}(B_N, E_l) + W_{SE}(B_N, E_l) = \gamma N \frac{B_N}{B_{N,max}} \quad (2)$$

where  $\gamma$  is the rate of nuclear spin loss via spin relaxation and diffusion,  $N$  is the number of nuclei in the QD,  $B_{N,max}$  is the maximum  $|B_N|$  corresponding to 100% polarized nuclear spins ( $\mu_B g_e B_{N,max} = 230 \mu\text{eV}$  in InP [24]).

Numerical solutions of the nonlinear equation Eq. 2 for values of parameters relevant to our experiment are shown in Fig. 3. The Overhauser field  $B_N$  (dots) and nuclear spin pumping rate  $|W_{pump}|$  at  $B_N=0$  are shown in panels (a) and (c) for  $B_z = 2.5$  T and  $B=0$  respectively. Calculated PL transition energies  $E_{\uparrow\downarrow\downarrow} - E_{\downarrow}$  and  $E_{\uparrow\downarrow\uparrow} - E_{\uparrow}$  are shown in panels (b) and (d) with symbols, and the pump laser energy is shown by the continuous lines.

The best description of the experiment is achieved with realistic parameters: nuclear polarization fluctuation  $\mu_B g_e \langle \delta B_N^2 \rangle^{1/2} \approx 1.53(1.05) \mu\text{eV}$ , electron spin level broadening  $\hbar/\tau \approx 6.8(5.5) \mu\text{eV}$  and excitation power is  $\Omega_R \tau \approx 2.0(3.5)$  at  $B_z=0(2.5)$  T. As expected, the best fits reflect the strong suppression of the nuclear spin depolarization rate in high magnetic fields:  $1/(\gamma N) \approx 2$  ns at  $B=0$  and increases up to  $\approx 1.4 \mu\text{s}$  at  $B_z=2.5$  T.

At high magnetic field the calculated behavior is in excellent agreement with the experimental data in Fig.2a,c: under  $\sigma^+$  polarized excitation switching to low  $|B_N|$  occurs towards high  $E_l$ , when  $E_l = E_{|\uparrow\downarrow\rangle} - E_{|\downarrow\rangle}$ , corresponding to the  $\sigma^+$  PL (allowed) transition. This process is described by  $W_{OE}$  in Eq. 2. As in experiment another abrupt switching to a markedly higher nuclear polarization is observed when the laser is tuned to the forbidden  $|\downarrow\rangle \rightarrow |\uparrow\downarrow\rangle$  transition, the process described by  $W_{SE}$ .

The origin of the asymmetric shapes of the resonances in Figs.2 and 3 lies in the non-linear dependence of the trion transition energies on the nuclear field  $B_N$ . As a consequence both the detuning from the laser and the nuclear spin pumping rate  $W_{pump}$  are also dependent on  $B_N$ . The highest nuclear spin pumping efficiency in both OE and SE processes is reached when the laser is in exact resonance with the  $|\downarrow\rangle \rightarrow |\uparrow\downarrow\rangle$  and  $|\downarrow\rangle \rightarrow |\uparrow\downarrow\rangle$  transitions, respectively. If in this condition the laser is tuned away from resonance  $|B_N|$  can only decrease. This leads to the shift of the  $|\uparrow\downarrow\rangle$  state involved in the OE process to lower energy. If the laser is tuned above resonance this shift leads to even larger detuning and lower nuclear spin pumping efficiency. Such feedback results in a quick collapse of  $|B_N|$ . If the laser is tuned to lower energy, the shift of the  $|\uparrow\downarrow\rangle$  level partly restores the resonant condition making the reduction in the nuclear spin pumping efficiency more gradual. In contrast to the OE case, the  $|\uparrow\downarrow\rangle$  trion state involved in the SE shifts to lower energy with the build-up of negative  $B_N$ . Thus the asymmetric shape of the SE resonance exhibits the sharp drop in  $|B_N|$  in the direction of low  $E_l$  [25].

Calculations for the case of  $B=0$  (Fig.3 c,d) also show an asymmetric resonance with the abrupt change in nuclear polarization on the low energy side, in agreement with the results in Fig.2. As in experiment, the abrupt increase of  $|B_N|$  under  $\sigma^+$  excitation is observed when the laser is in exact resonance with the  $\sigma^-$  PL line (transition to  $|\uparrow\downarrow\rangle$  state), demonstrating efficient nuclear spin pumping through the forbidden optical transition.

According to Eq.1  $W_{OE}$  reaches a maximum value of  $W_{OE}^{max} = \alpha^2 \tau^{-1} / 2$  when the allowed transition saturates ( $\tau \Omega_R \gg 1$ ). By contrast, the maximum  $W_{SE}^{max} = \tau^{-1} / 2$  is limited only by the radiative lifetime of the trion,  $\tau$ , and exceeds  $W_{OE}^{max}$  in a wide range of magnetic fields by  $\alpha^{-2} > 3000$  [26]. According to Eq.1  $W_{SE}$  also saturates at much higher laser power ( $\alpha \tau \Omega_R \gg 1$ ) than  $W_{OE}$ . By performing power-dependent measurements, we find that the maximum nuclear polarization pumped via the allowed transition increases with power and saturates at 45%. For pumping via the "forbidden" transition, we obtain a maximum nuclear polarization of 65%, 1.5 and 1.2 times higher than the saturation levels observed for the OE cycle and non-resonant excitation, respectively. Surprisingly, the saturation of the pumping via the "forbidden" transition occurs at a similar power to the OE case. We thus conclude that the saturation of  $|B_N|$  is not

due to saturation of the forbidden transition itself. These results of the power-dependence (to be reported in detail elsewhere) suggest that the complete physical picture of the observed phenomena should also include additional mechanisms such as, for example, decreasing availability of unpolarized nuclei or formation of dark nuclear states [16, 17] in the dot. Such processes, yet to be fully understood, may set a fundamental limit to the efficiency of the optical orientation of nuclear spins.

In conclusion, we have employed resonant pump-probe techniques to demonstrate the "optical solid effect" based on optically forbidden transitions in a positively charged quantum dot. This phenomenon results in efficient nuclear polarization over a wide range of finite and zero magnetic fields. Using model calculations based on optical Bloch equations we show that interaction of the laser with both allowed and forbidden QD transitions is significant, and find that in realistic conditions the forbidden process is the most efficient mechanism of dynamic nuclear polarization.

Since submission of our manuscript, related work on resonant pumping of negatively charged dots has been published [27].

We are grateful to V. I. Fal'ko, A. J. Ramsay, V. L. Korenev and V. D. Kulakovskii for fruitful discussions. This work has been supported by the EPSRC grants EP/G601642/1, EP/C54563X/1, the EPSRC IRC for QIP, and the Royal Society.

- 
- [1] H. Haffner *et al.*, Nature **438**, 643 (2005).
  - [2] C. Santori *et al.*, Phys. Rev. Lett. **97**, 247401 (2006).
  - [3] M. Atature *et al.*, Science **312**, 551 (2006).
  - [4] M. H. Mikkelsen *et al.*, Nature Physics **3**, 770 (2007).
  - [5] B. D. Gerardot *et al.*, Nature **451**, 441 (2007).
  - [6] D. Press *et al.*, Nature **456**, 218 (2008).
  - [7] A. J. Ramsay *et al.*, Phys. Rev. Lett. **100**, 197401 (2008).
  - [8] X. Xu *et al.*, Phys. Rev. Lett. **99**, 097401 (2007).
  - [9] D. Brunner *et al.*, Science **325**, 70 (2009).
  - [10] X. Xu *et al.*, Nature **459**, 1105 (2009).
  - [11] A. V. Khaetskii, D. Loss, L. Glazman, Phys. Rev. Lett. **88**, 186802 (2002).
  - [12] V. K. Kalevich, K. V. Kavokin, I. A. Merkulov, in *Spin Physics in Semiconductors* edited by M. I. Dyakonov, (Springer, 2008).
  - [13] D. J. Reilly *et al.*, Science **321**, 817 (2008).
  - [14] J. R. Petta *et al.*, Science **309**, 2180 (2005).
  - [15] A. Greilich *et al.*, Science **313**, 341 (2006).
  - [16] H. Ribeiro and G. Burkard, Phys. Rev. Lett. **102**, 216802 (2009).
  - [17] A. Imamoglu *et al.*, Phys. Rev. Lett. **91**, 017402 (2003).
  - [18] V. L. Korenev, Phys. Rev. Lett. **99**, 256405 (2007).
  - [19] A. Abragam, M. Goldman, Rep. Prog. Phys, **41**, 395 (1978); A. Abragam, *The principles of Nuclear Magnetism* (Oxford University Press, London, 1961).
  - [20] A. S. Bracker, D. Gammon, V. L. Korenev, Semicond. Sci. Technol **23**, 114004 (2008).

- [21] A. I. Tartakovskii, *et al.*, Phys. Rev. Lett. **98**, 026806 (2007).
- [22] B. Urbaszek, *et al.*, Phys. Rev. B **76**, 201301(R) (2007).
- [23] J. Skiba-Szymanska *et al.*, Phys. Rev. B **77**, 165338 (2008).
- [24] B. Gotschy, B. Denninger, H. Obloh, W. Wilkening, J. Schneider, Solid State Commun. **71**, 629 (1989).
- [25] Metastable nuclear spin states are observed in experiment and will be reported elsewhere. Relevant theory results are shown in Fig.3(a).
- [26] The forbidden transition was not observed in PL measurements, which taking into account the signal-to-noise ratio in PL provides the upper estimate for  $\alpha^2 < 1/3000$ .
- [27] C. Latta *et al.*, Nature Physics advance online publication 16 August 2009 (doi:10.1038/nphys1366).